2016

An Investigation of AMS in Oman Ophiolite Gabbros

Sarah D. Trutner
Oberlin College

AN INVESTIGATION OF AMS IN OMAN OPHIOLITE GABBROS

Sarah D. Trutner
Advisor: Andrew J. Horst

Honors Thesis
Oberlin College Geology Department
April 2016

Abstract

Crustal accretion processes at mid-ocean ridges are still poorly understood, and several competing models exist that try to explain exactly how magma from the mantle is incorporated into oceanic crust at a crustal spreading center. Ophiolites, or fragments of oceanic crust exposed on land, are useful sites at which to conduct rock fabric studies to understand oceanic crust formation processes. This study focuses on samples of upper foliated gabbros taken from the Oman ophiolite in order to characterize their fabric orientations and contribute to a better model of crustal formation. Much of the focus of this study is on using and interpreting anisotropy of magnetic susceptibility (AMS) as a method for measuring rock fabric directions. From our study site near the Maqsad diapir on the Sumail Massif, we found a magnetic foliation oriented NW-SE, subparallel to the nearest inferred spreading ridge and dipping steeply to the SW. The magnetic lineation from most of our samples was plunging moderately to the NW, towards the diapir. Comparison with shape-preferred orientation (SPO) measurements and other magnetic experiments indicate that our AMS fabrics match well with crystal fabrics, at least in foliation direction, and the magnetic susceptibility of our samples is largely due to secondary magnetite in serpentinized olivine.

Table of Contents

1. Introduction

Although oceanic crust constitutes the majority of Earth's lithosphere, the processes of its formation at oceanic spreading centers are poorly understood, especially in the middle to lower part of the crust. Unfortunately, it is often infeasible to study the entire formation process as it occurs at a spreading center, due to the difficulty of both retrieving samples from the seafloor and directly observing magmatic processes underneath the crustal surface. Magma transport mechanisms in middle to lower oceanic crust can be better understood by studying the mineral foliations and lineations that form as the crust freezes, since this alignment, or fabric, is thought to accurately record the direction of magma flow (Yaouancq and MacLeod, 2000). Some progress has been made by using geophysical techniques to understand subsurface activity, since seismic studies are useful for understanding subsurface structures (Sinton and Detrick, 1992; Collier and Singh, 1997; Nicolas et. al., 2009), and can detect crystal alignments through seismic anisotropy in some cases. However, even seismic studies are only so useful if there is no way to directly interpret the data, so it is still necessary to have ways to characterize the actual fabric and structures of the oceanic crust (Christensen and Smewing, 1981).

Luckily, there are opportunities to directly study oceanic crust at ophiolites. As fragments of oceanic crust obducted onto a continent, ophiolites preserve a record of their formation on the seafloor. While that record can in some cases be altered and deformed, the fact that it is exposed on land makes it possible to directly study the lower oceanic crust. In some large ophiolites, it is possible to see the entire

crustal sequence, including peridotites in the upper mantle, gabbros in the lower and middle oceanic crust, and sheeted dike complexes to pillow basalts in the upper crust. Multiple petrofabric studies have been done on foliated gabbros just below the sheeted dike complexes in ophiolites to take advantage of their exposure and accessibility (Boudier et. al., 1996; Yaouancq and MacLeod, 2000; Abelson et. al., 2001; Kawamura et. al., 2005; Granot et. al., 2011; Archanjo et. al., 2012; VanTongeren et. al., 2015).

Rock fabric studies can be undertaken with several different methods, and each one has its pros and cons. Fabric studies based on microscopic crystal orientations tend to give reliable results with sufficient data, but they do have some drawbacks. Along with any observations made in the field, fabric data must be collected from thin sections of the ophiolite samples. Thin sections only give a small, 2-dimensional view of the sample, so 3-dimensional data must be calculated by looking at multiple thin sections, usually a set of 3 orthogonal slides. There is likely some error associated with the fact that cutting thin sections is a destructive method of studying a sample, so the orthogonal sections may be sourced from nearby points, but may not be from the same sample.

Anisotropy of magnetic susceptibility (AMS) is an alternate method for petrofabric studies that is much less prone to the drawbacks described above. AMS is a nondestructive method of measurement that determines a directional fabric ellipsoid from a sample by measuring its magnetic response to a field in various directions. With the computational methods available today, it can be measured on a sample and recorded as a 3-dimensional output within a couple of minutes, making

it very convenient to use. It is also applicable to a variety of geologic studies, since all materials have some type of magnetic response, and fabric studies are useful for igneous, metamorphic, and sedimentary rocks (Tarling and Hrouda, 1993).

Along with other rock fabric measurement methods, however, the interpretation of AMS data is often complicated. Because different minerals have varying responses to a magnetic field (i.e. are diamagnetic, paramagnetic, or ferromagnetic), the AMS of a rock depends on which types of magnetism dominate the signal. Ferromagnetic minerals like magnetite are found in many different environments and have a much stronger magnetic response than paramagnetic or diamagnetic materials, so they can swamp the magnetic susceptibility of a sample if they are present, even in small amounts (Tarling and Hrouda, 1993). However, crystals of ferromagnetic minerals can have varying magnetic behavior, depending on their size and composition. Thus, the reliability and correct interpretation of AMS results depend on a more detailed understanding of the rocks being studied.

This project focuses on developing a detailed, small-scale understanding of samples taken from foliated gabbros in the Oman ophiolite and their AMS fabrics. Some of the existing models for oceanic crust formation will be described, along with the basis for AMS measurements and factors that complicate their interpretation. Our methods to understand the origin of the AMS signal in our gabbro samples will then be discussed, along with patterns seen in the results and the implications for other studies on gabbros in the Oman ophiolite.

2. Background

2.1. Site Geology

The Oman ophiolite is located in the Al Hajar Mountains in northern Oman (Figure 1). According to previous studies, it originally formed in a spreading center 96-94 Ma, and was obducted onto the Arabian continental margin by the end of the Cretaceous period, 65 Ma (Searle and Cox, 1999). The ophiolite is generally believed to have originally formed at a fast-spreading oceanic ridge (Keleman et. al., 1997); however, plenty of debate still exists around whether it formed instead in an island arc above a subduction zone (Searle and Cox, 1999; MacLeod et. al., 2013). Its structure includes lower layered gabbros, upper foliated gabbros, sheeted dike complexes, and pillow lavas overlain by marine sediments. Sequences like this one in ophiolites around the world have been used to understand the structure of oceanic crust, as studying the lower crust directly is infeasible due to the necessity of dealing with both the overlying rock and its location on the seafloor.

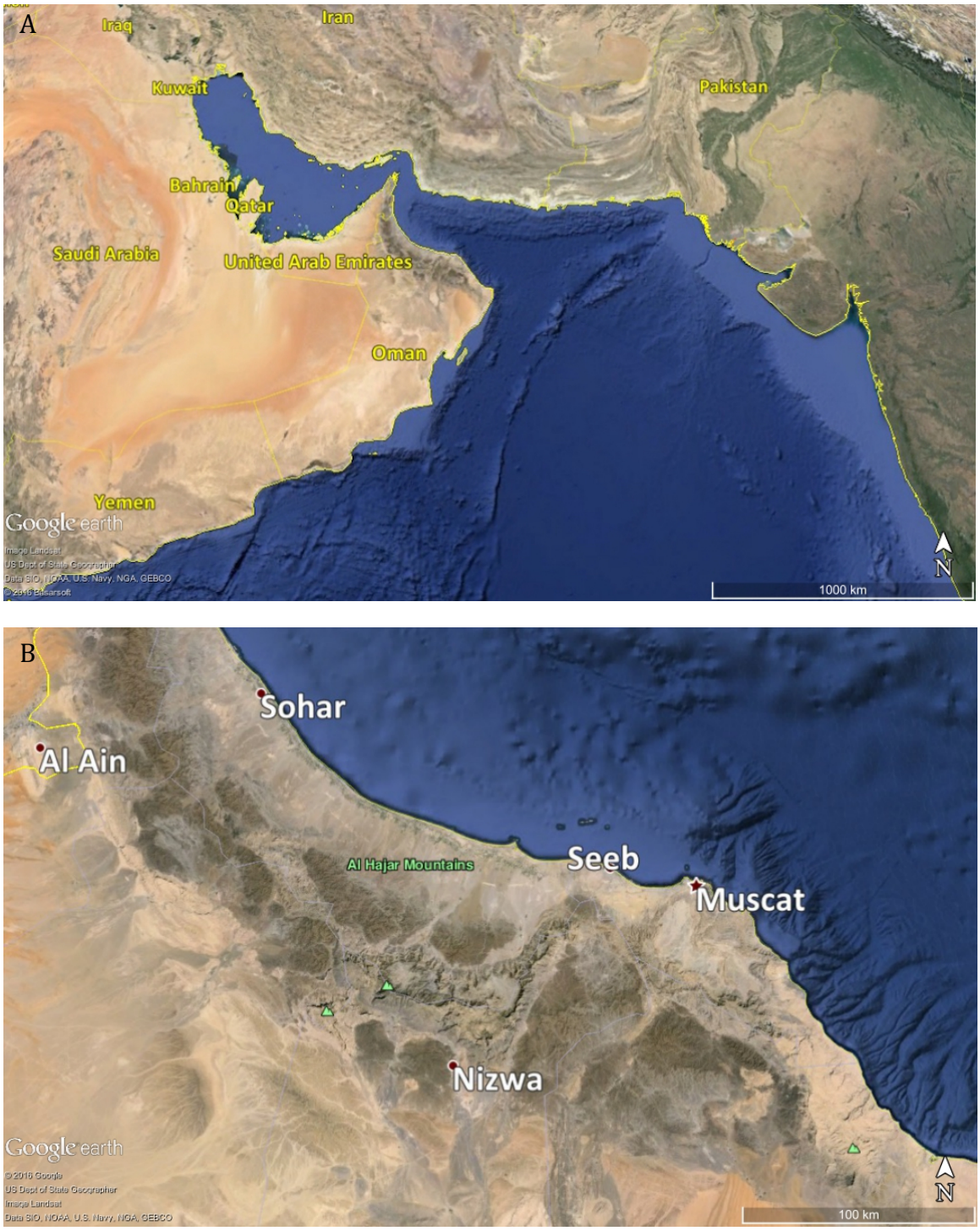

Figure 1: Two Google Earth images showing the general location of the Oman ophiolite. A: The Gulf of Oman and the countries that surround it. B: A more zoomed in image of the Al Hajar Mountains, which coincide with the shape of the ophiolite. The ophiolite itself is visible from satellite imagery because it is visibly darker than the surrounding land. This project focuses on the Samail Massif, which is located in the southeastern area of the ophiolite.

The transition between the foliated gabbros and the sheeted dike complex in oceanic crust is an area of great interest, as the gabbros are foliated with varying attitudes, but the sheeted dikes are near vertical. Ophiolites like the one in Oman have been the focus of extensive rock fabric studies, as understanding the flow directions in the normally inaccessible lower crust is much more doable from a surface exposure.

Recent studies of mid-ocean ridges have concluded that much of the crust is formed at an axial melt lens located near the root zone of the sheeted dike complex. The lens is located about 1-3 km below the seafloor and extends outward about 1 km in each direction from the ridge axis. There appears to be some disagreement about exactly how thick the lens is, but it could be either about 50 m or 200-300 m thick (Collier and Singh, 1997; Sinton and Detrick, 1992). One of several existing models that attempt to explain the formation of lower oceanic crust suggests that the gabbros below the melt lens may form as the melt subsides, creating a steep foliation by the time the rock fabric freezes in the crust (Figure 2a). That fabric would then be detectable in the resulting oceanic crust even after it moved outward from the ridge (Nicolas et. al., 2009). However, it is unclear how this subsidence would interact with magma moving upward toward the ridge, and others have argued that magma instead generally moves up from the crust-mantle boundary toward the axial melt lens and sheeted dikes, perhaps in a series of sills (Keleman et. al., 1997). A newer study (VanTongeren et. al., 2015) also discusses this "sheeted sills" model in contrast to the "gabbro glacier" model of subsidence down from the axial melt lens (Figure 2b). It is evidently still not clear which of these models most

accurately describes the process of oceanic crustal accretion, so more detailed fabric studies are necessary to fully characterize oceanic crustal fabrics and understand the magmatic processes that formed them.

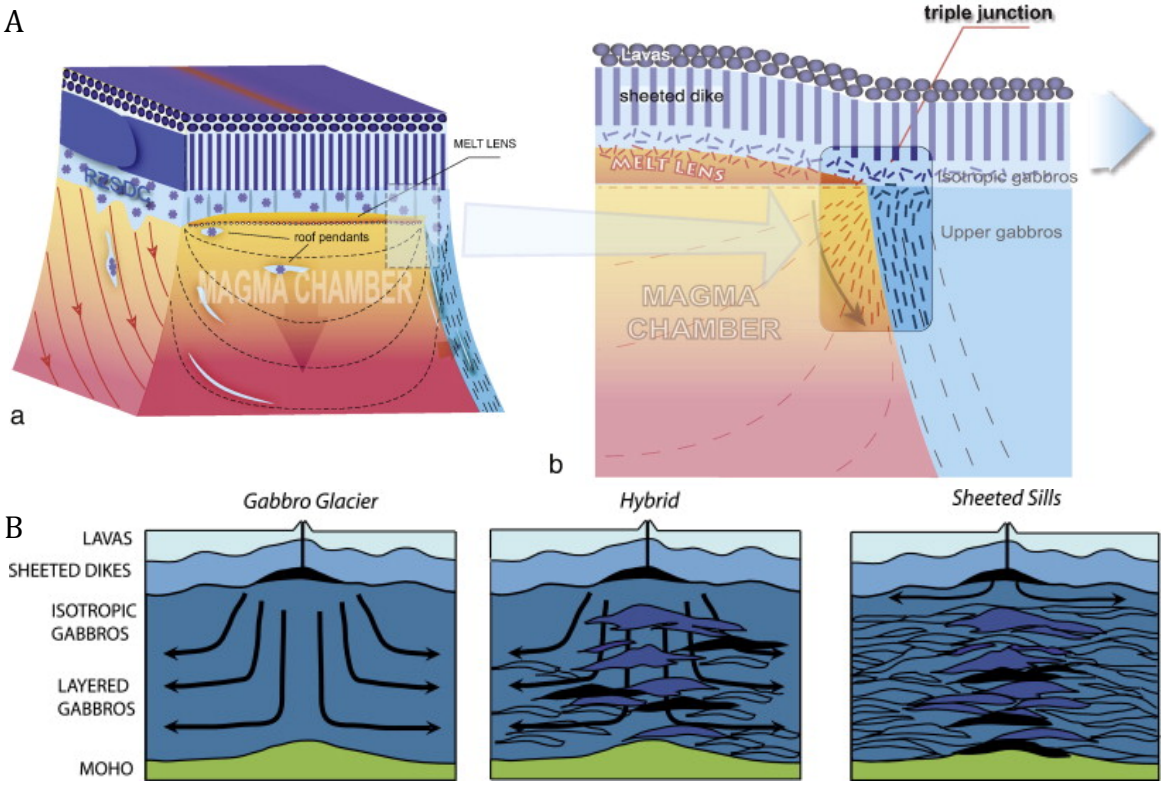

Figure 2: A, taken from Nicolas et. al., 2009, showing one possible model for how the fabric in foliated gabbros is formed. In this model, the axial melt lens (just above the magma chamber) steadily subsides as it crystallizes. This subsidence causes the resulting gabbro foliation to align in a U-shape, becoming horizontal near the bottom of the gabbro section and subvertical near the top. B, taken from VanTongeren et. al., 2015, shows the contrast between the competing "gabbro glacier" model and "sheeted sills" model, with a hybrid option in which sills are periodically emplaced into a downward-flowing crystal mush.

2.2. AMS

Anisotropy of Magnetic Susceptibility (AMS) is a measurement of how an object's magnetization changes as a function of the direction of an applied magnetic field, and is a useful method for characterizing rock fabrics. When a rock is placed in a magnetic field, its magnetization is dependent on both the strength of the field and the magnetic susceptibility of its constituent minerals. However, if the field strength

is kept constant but its direction through the rock changes, variations in the rock's magnetization (and thus its susceptibility) can be recorded. The results can be visualized as an ellipsoid (Figure 3), with the axes Kmax, Kint, and Kmin representing the directions of maximum, intermediate, and minimum susceptibility, respectively. Magnetic susceptibility is strongly affected by how much material a field is going through in a given direction. In multi-domain elongate or needle-shaped magnetic crystals, Kmax tends to match the direction of the long axis. If multiple crystals align in the same direction, as they do in the development of a foliation or lineation, that alignment can theoretically be detected in the AMS of a sample that contains it. In igneous rocks, the principal direction (Kmax) of the AMS ellipsoid corresponds to the flow direction of the source magma as it was cooling (Hrouda, 1982).

When relying on AMS for information about igneous rock fabric, it is important to check where the signal is actually coming from, as processes outside of the original flow direction can change the magnetic fabric direction and make any interpretations based on it unreliable. The signal can be changed by deformation, secondary mineralization, and exsolution, along with other processes that affect the size shape of magnetic grains within a rock. Most of these characteristics are measurable, so AMS data can be paired with other magnetic measurements and observations of visual and chemical characteristics to trace the source of the signal and see how well the magnetic fabric should match with the silicate fabric.

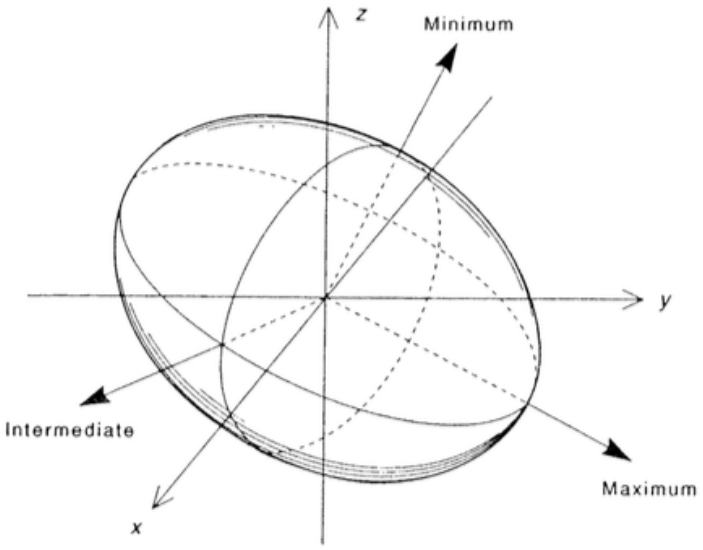

Figure 3: A visual representation of an AMS ellipsoid. K maximum, or Kmax, defines the direction of maximum susceptibility in the sample. K minimum and K intermediate (Kmin and Kint) define the direction of minimum susceptibility and the direction orthogonal to both the maximum and minimum, respectively.

3. Methods

3.1. Fieldwork

Samples were collected from the Sumail Massif of the Oman ophiolite in January 2015 (Figure 4). This project will focus on 260 samples taken from 18 sites in the upper foliated gabbros. Multiple cores were taken at each site with a drill, and several sets of cores were taken across or along certain foliated zones in order to examine any change in magnetic fabric (Figure 5). Mesoscopic foliations defined by the alignment and layering of plagioclase, pyroxene, and olivine was visible in the field, so the orientations of those foliations were recorded for later comparison with AMS and crystal fabrics. However, mineral lineations were either not visible or were obscured by desert varnish.

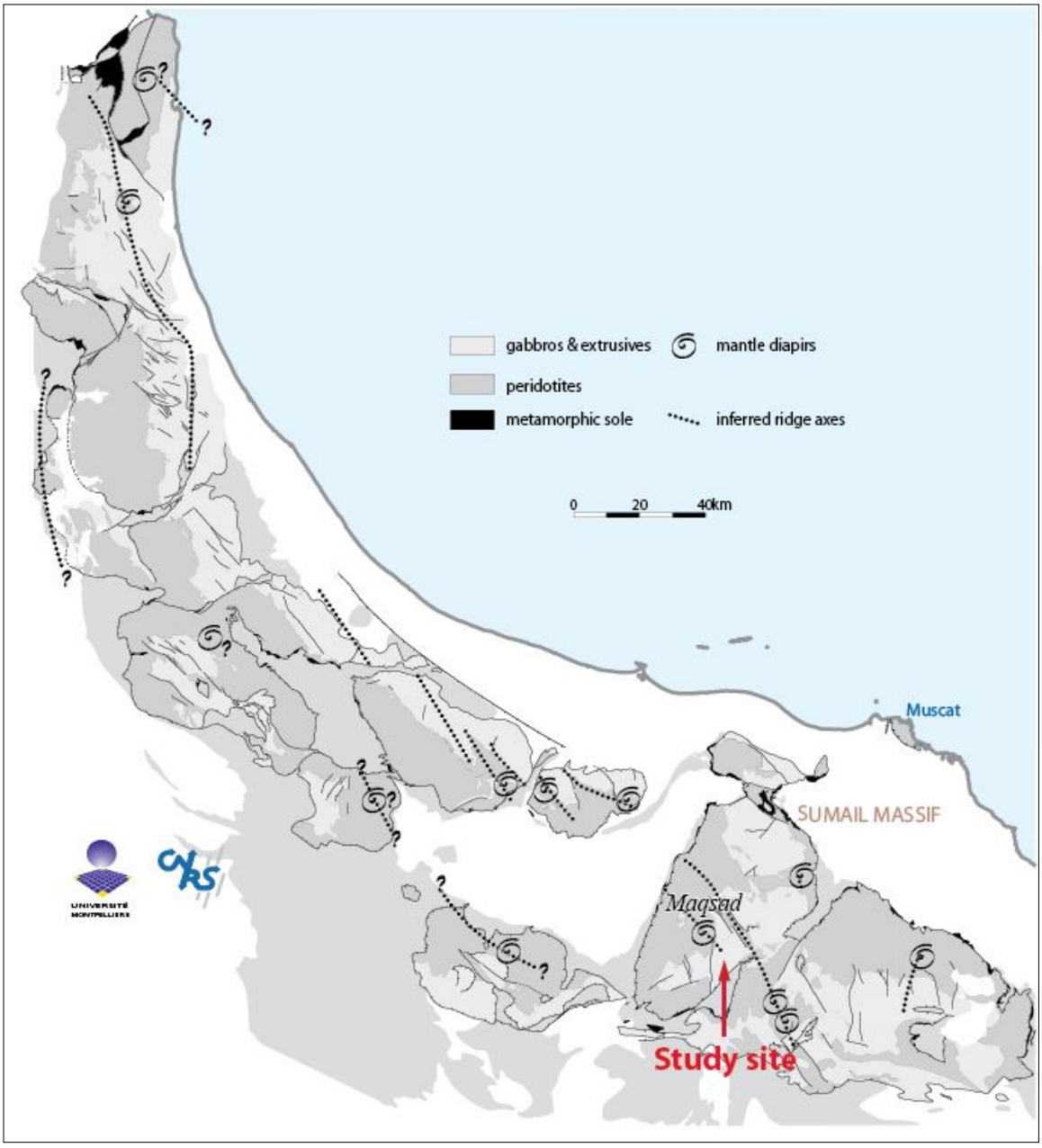

Figure 4: Geologic map of the Oman ophiolite, including the location of our study site on the Sumail Massif, in the southern section of the ophiolite. The site is southeast of the Maqsad diapir, a probable fossil source area of magma from the mantle, and immediately south of an inferred spreading ridge axis. Figure altered from Nicolas et. al., 2009.

Figure 5: Pictures of drill locations and mesoscopic foliations at sites 4 and 5 (left, respectively along and across the foliation) and 10 (right). More cores for site 4 were taken outside the view of the photo. Cores for each site were taken either moving across visible foliation, as shown here, or along a particular foliation plane. Each core is about 2.5 cm wide. Both views are towards the southeast.

3.2. Anisotropy of Magnetic Susceptibility (AMS)

The 2.5 cm diameter cores were taken to Scripps Institute of Oceanography in San Diego in July 2015. There, they were cut into samples about 2.4 cm in length to be measured for AMS. Prior to any other magnetic procedure, each sample was placed in an AGICO KLY-4S Kappabridge and rotated around each of the three sample coordinate axes in a field of 300 A/m. Directional susceptibility values were recorded at 64 points during each axial revolution for a total of 192 susceptibility measurements. A program created at Scripps, called AMSSpin, was then used to calculate the 3D susceptibility tensor and record the three principal axes for the AMS ellipsoid (Gee, 2008). This measurement process was done on all of our samples.

3.3. Low-Temperature Magnetization

The samples were then taken to the Institute for Rock Magnetism in the University of Minnesota, Minneapolis. There, several other experiments were done on selected samples from each site. The IRM has two Magnetic Properties

Measurement System (MPMS) instruments, built by Quantum Design, Inc., which are capable of measuring magnetic remanence as it varies with low temperature. The instruments are capable of performing a wide variety of experiments. We used the MPMS-5S model and performed a measurement sequence on our samples called "Sweep-Cool-Warm", in which a sample is given a magnetization in a 2.5 T field at room temperature, cooled to a specific temperature (here, 20K) in zero field, given another magnetization in 2.5 T, and warmed back up to room temperature in zero field. The magnetic remanence is measured at every 5 K interval (Bilardello and Jackson, 2013). This experiment is useful for identifying specific magnetic minerals in a sample, as certain minerals will undergo a crystallographic shift and lose magnetization at specific temperatures. Pure magnetite, for example, shifts from a cubic to a monoclinic crystal lattice at 120K. We performed MPMS experiments on one sample from each site in order to characterize the magnetic minerals that were common in the gabbros and see whether those minerals varied from site to site.

3.4. High-Temperature Susceptibility

We also did thermal susceptibility experiments on a sample from each site. Thermal susceptibility is also useful for identifying magnetic minerals, but is measured while heating the sample, rather than cooling it as in MPMS experiments. It is done by heating a powdered sample to about 700°C and cooling it back down to room temperature in argon atmosphere, while measuring the bulk susceptibility of the sample in a 300 A/m field every 30 seconds. The resulting heating and cooling curves are indicative of whatever magnetic minerals are present, as different minerals lose their susceptibilities above different temperatures; these are the

points at which thermal energy is higher than magnetic energy and the material cannot have a magnetization, even in a small field (Tauxe et. al., 2014). If the shapes of the cooling and warming curves are different, or if susceptibility rises at all while the sample is warming, that may also give clues about exactly what minerals are present. Like the MPMS experiments, the thermal susceptibility measurements helped us to characterize the presence of magnetic minerals in each sampling site.

3.5. Hysteresis

Hysteresis loops are useful for determining the type of magnetism (e.g. paramagnetism, ferrimagnetism, etc.) and general size of magnetic grains contained in a given sample. A hysteresis loop is measured in a vibrating sample magnetometer (VSM), which applies a magnetic field to a sample and measures its magnetic moment parallel to the field as a function of the field strength. Paramagnetic materials show a linear increase in magnetic moment as the field increases, while ferromagnetic materials change rapidly in lower fields and level off in higher fields as they reach saturation. Because ferromagnetic materials are capable of holding remanent magnetizations, previous saturation values have an effect on low-field magnetic moments and the full experiment (which involves going to a saturation field in opposite directions) creates a loop rather than a single curve. The shape of the loop gives four values that can then be used to find the general magnetic grain size. The saturation magnetization Ms is the maximum moment value that the sample holds once the paramagnetic slope is accounted for, and is measured at a high field. The saturation remanence Mr is the moment that the sample retains after being saturated; this is measured at zero field. When a field

applied in the opposite direction brings the sample magnetization to zero, that field is called the bulk coercive field, Hc. The field that, when reduced to zero, leaves zero net remanence after the sample was saturated in the opposite direction is called the coercivity of remanence, Hcr. These values can then be used to define the crystals in the sample as single-domain (SD), multi-domain (MD), or pseudo-single-domain (PSD). For example, using the boundaries in a Day diagram (Day 1977), samples whose Mr/Ms and Hcr/Hc ratios fall in the box $0.05 < Mr/Ms < 0.5$ and $1.5 < Hcr/Hc < 5$ are considered to be PSD. This is by far the most common result for rock magnetic hysteresis experiments, as samples rarely contain either purely single-domain or multi-domain crystals and mixtures tend to have PSD-like behavior (Tauxe et. al., 2014).

3.6. Shape-Preferred Orientation (SPO)

Most of these experiments were done with the intent to characterize the magnetic minerals and grain sizes present in the samples and find the sources of the magnetic signal that we had measured in the earlier AMS experiments. In order to make sure that the AMS was reliable, we also used optical methods of finding rock fabric directions and characterizing the minerals in the samples. After getting back to Oberlin, we chose 3 sites (5, 10, and 15) from which to calculate shape-preferred orientation (SPO) fabric directions. 3 orthogonal thin sections were made from each site and scanned with polarizing film. ImageJ was then used to threshold the images and find the 2D crystal fabric direction on each section. We then used a program to calculate the visual fabric ellipsoid from the 2D data (Gee, 2004), and compared that with the AMS ellipsoid data for that site (Figure 6). The orthogonal thin sections, as

well as individual thin sections selected from other sites, were also examined using a petrographic microscope with both transmitted and reflected light in order to examine the minerals and textures present in the samples.

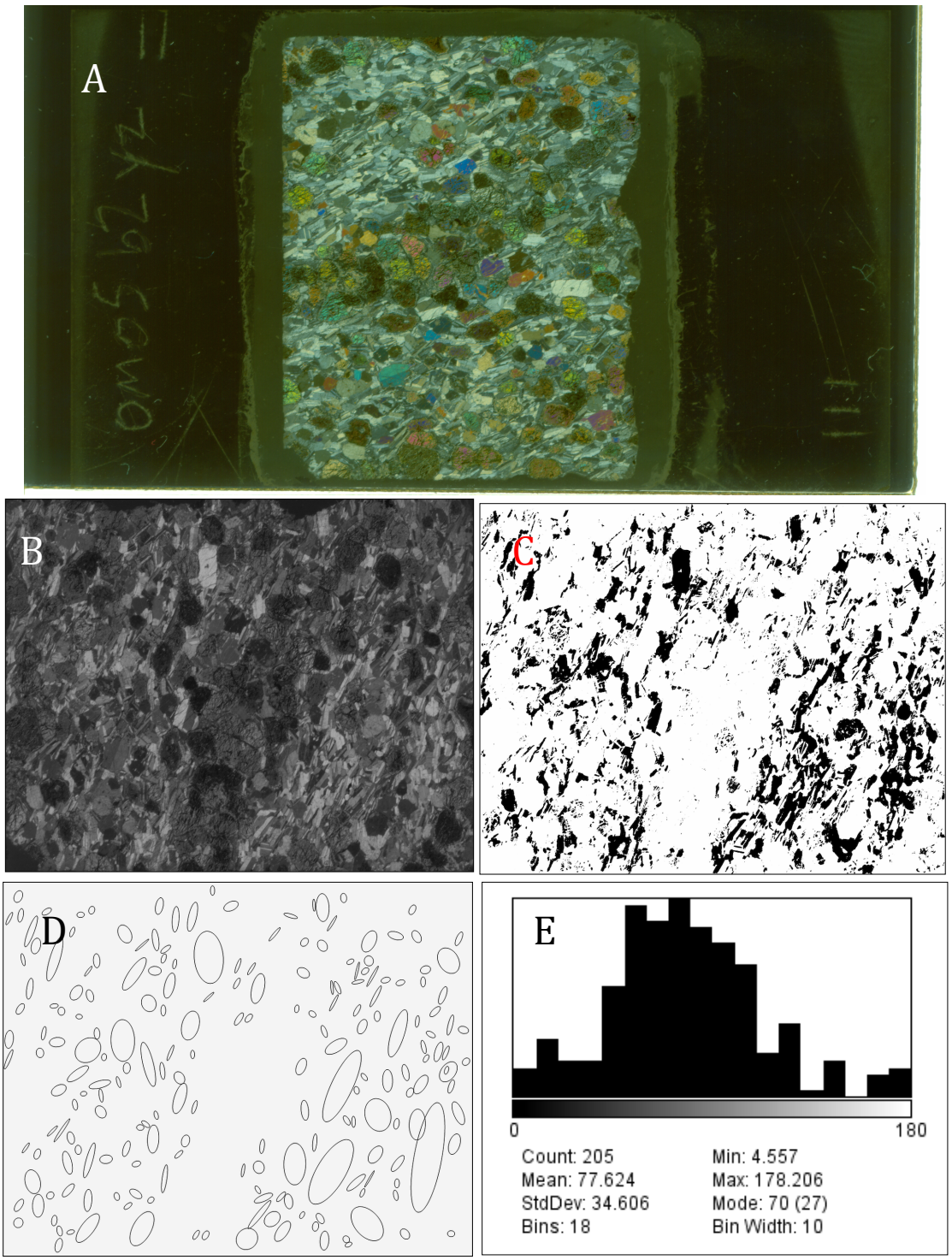

Figure 6: Example images from the SPO calculation process. A) A scanned image of a thin section in between two orthogonally oriented pieces of polarizing film. +Y is up and +Z is to the right. B) A cropped, 8-bit version of image A. The image is rotated and flipped so that +Y is to the right and +Z is up. C) Image B, inverted and thresholded so that the originally lighter plagioclase crystals showed up as black. D) Ellipse representations of ImageJ's shape measurements of image C. E) A histogram showing the angles in which the ellipses are oriented. 0 degrees matches with +Y, on the right side of the previous three images. Angles are counted counterclockwise. This data, along with similar data from the XY and XZ thin sections for this site, were then used to calculate 3-dimensional rock fabric directions.

3.7. Scanning electron microscope (SEM)

We also used Oberlin's scanning electron microscope (SEM) to more accurately characterize the minerals, magnetic and otherwise, of the samples. We carbon-coated certain thin sections once they had been scanned and put them in the SEM to see the mineral boundaries and find where the magnetic minerals were actually located within the samples. We also used backscattered electron (BSE) imaging to find the compositions of the various minerals to verify those that we found in thin section and identify the ones that we had not been able to identify definitively, which were mostly opaques.

4. General Results

4.1. AMS and Crystal Fabrics

Our AMS data was fairly well-clustered in most cases, and the Kmax-Kint planes were similar to both the foliation attitudes observed in the field and the orientation of the nearby inferred ridge axis, with some exceptions (Figure 7). Sites with more variable results included 1, 3, 9, 14, 16, and 18, while the rest had very consistent axis directions and minimal scatter from individual sample results. Individual site results are discussed further below.

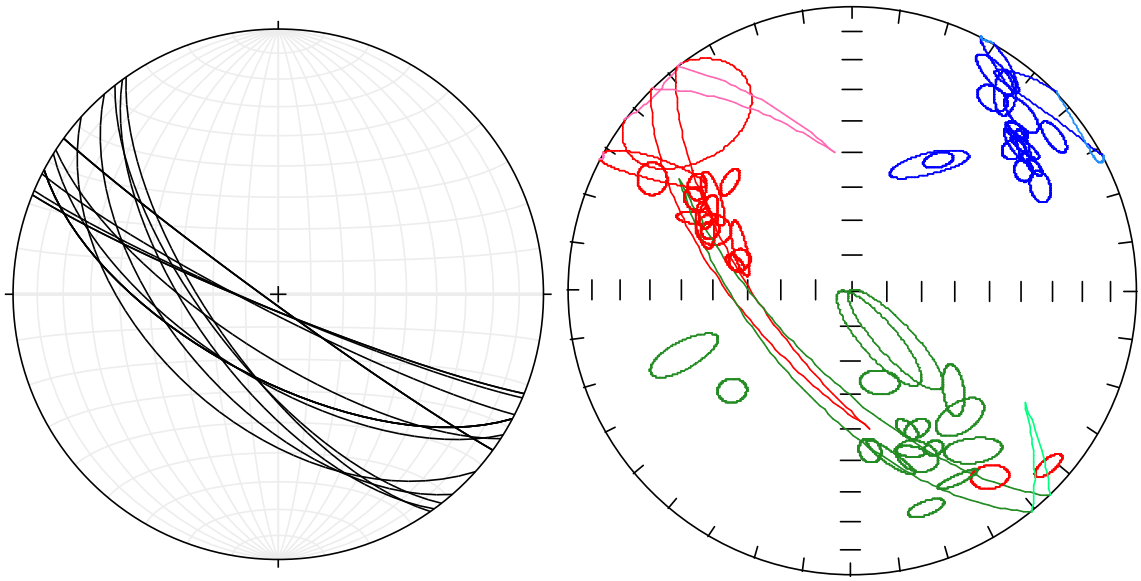

Figure 7: Foliation directions and AMS results from all 18 drill sites in geographic coordinates (North is up). A) The dips vary from moderate to steep, but all dip directions point generally towards the southwest. B) Red represents Kmax directions, green Kint, and blue Kmin. The Kmax and Kint directions together define the magnetic foliation, which matches well with both the foliations observed in the field and the trend of the inferred spreading ridge shown near our study site in Figure 4. The bootstrapped 95% confidence ellipses tend to cluster together very closely, with some visible exceptions. These will be discussed later. Site averages have been omitted for clarity.

When we compared plagioclase preferred orientation directions with the AMS data, we saw that the results were very similar, especially for the Kmin directions (blue circles), but the directions for Kmax (red squares) and Kint (green triangles) did not necessarily seem particularly close. When the maximum and intermediate axes are very similar or interchangeable, the fabric ellipsoid is referred to as oblate, meaning that a foliation or plane is more clearly traced out than a lineation. A mesoscopic foliation was observed in the field, and the data here do align such that the Kmax and Kint directions tend to fall on or near the recorded foliation planes. A lineation was not observed in the field, but our AMS data consistently indicated triaxial fabric shapes, meaning that there is both a magnetic foliation and a magnetic lineation. The lineation (Kmax) directions were also often very consistent between sites in our data. However, the direction of the magnetic

lineation does not appear to be supported by the data from our thin sections quite so consistently, so its significance is unclear (Figures 8-10).

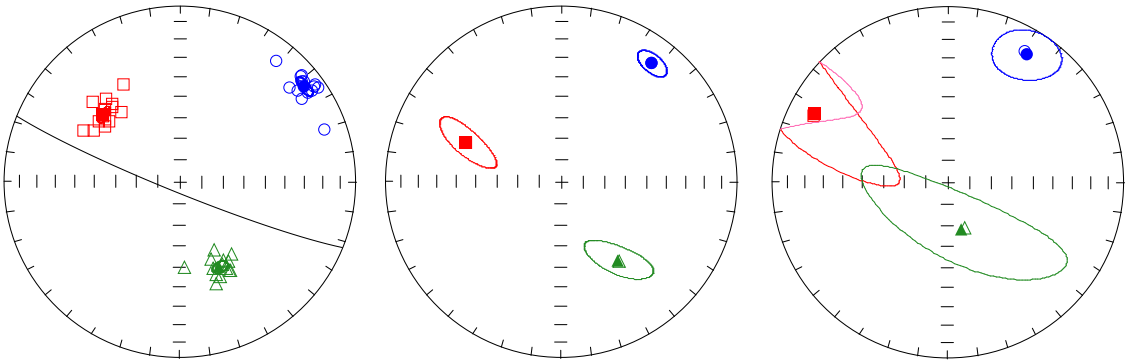

Figure 8: AMS and SPO data from site 5. The AMS data (left) appears to match very well with the SPO data from plagioclase and opaque mineral orientations (middle and left, respectively), as all three sets of axes are pointing in the same directions, with overlapping error ellipses.

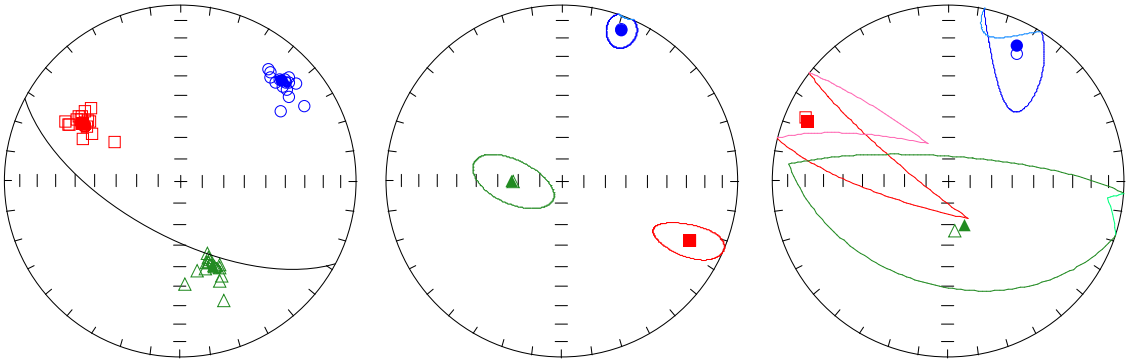

Figure 9: AMS and SPO data from site 10. Although the Kmin direction is roughly the same in each plot, the Kmax and Kint directions only seem to match between the AMS (left) and opaque (right) data. The plagioclase data (middle) seems to have its Kmax and Kint directions flipped or rotated from those of the AMS.

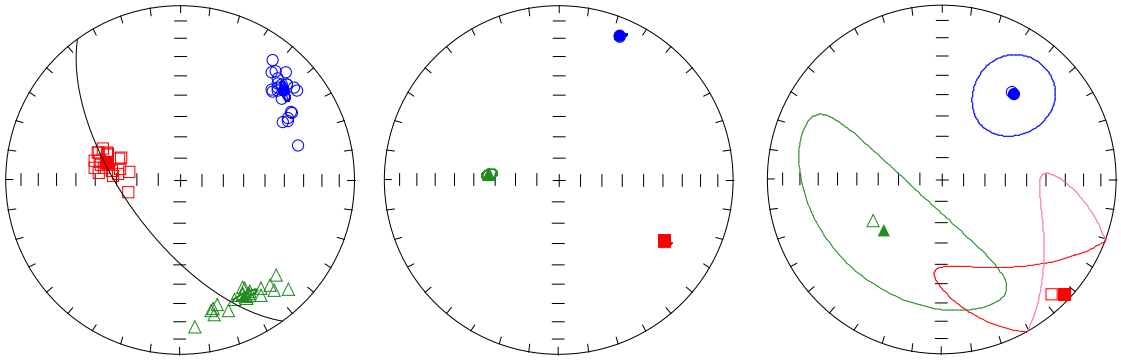

Figure 10: AMS and SPO data from site 15. Like site 10, the AMS and SPO data do not perfectly match, as their Kint and Kmax axes appear to be flipped. This does still indicate that the AMS data is showing roughly the correct foliation direction, but the magnetic lineation that it shows may not be real.

4.2. Low-Temperature Magnetization

In most of the samples that we tested with the MPMS, our results showed a clear loss of magnetization that centered at around 120K (Figures 11 and 12). This transition showed that there was magnetite present in these samples, which was most likely the largest contributor to our AMS signal. The degree of magnetization and the level of magnetization lost to the transition was not the same in all the results, which suggested varying amounts of magnetite present in the samples we used. Some results did not even show a visible transition at 120K, indicating that a few of our sites may have had little or no magnetite present (Figure 13).

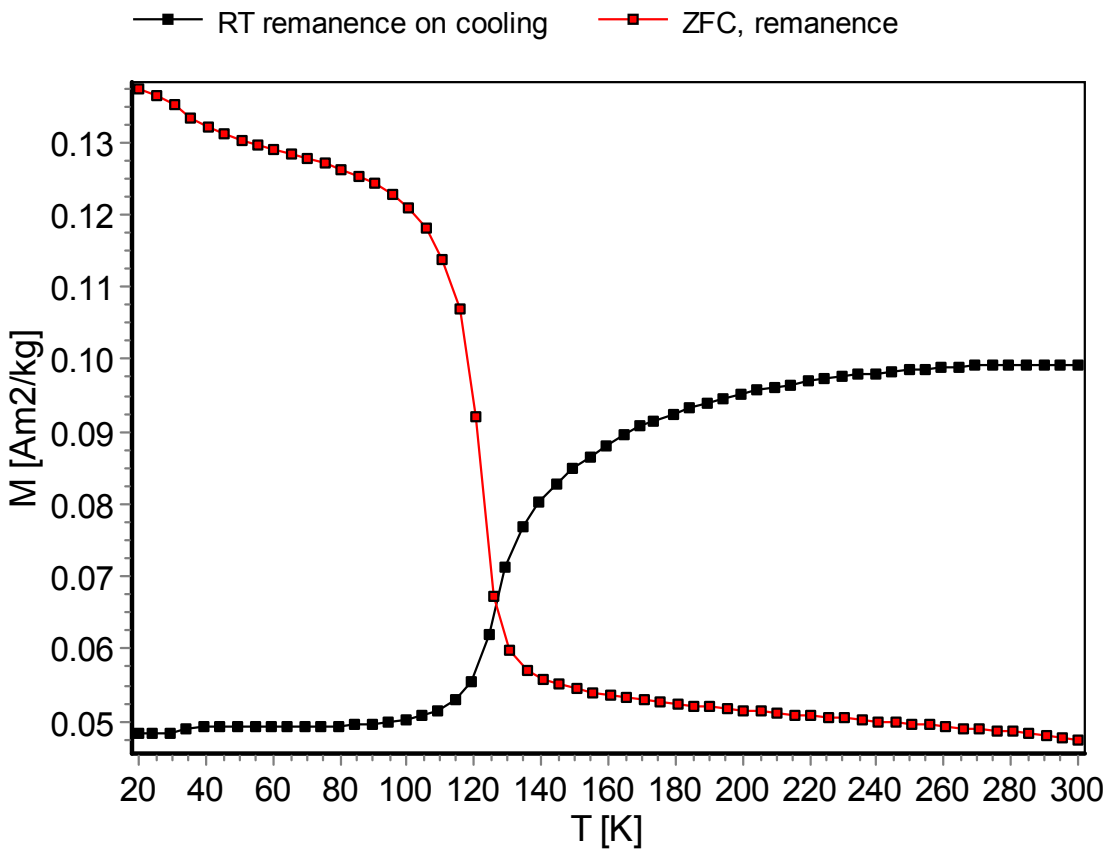

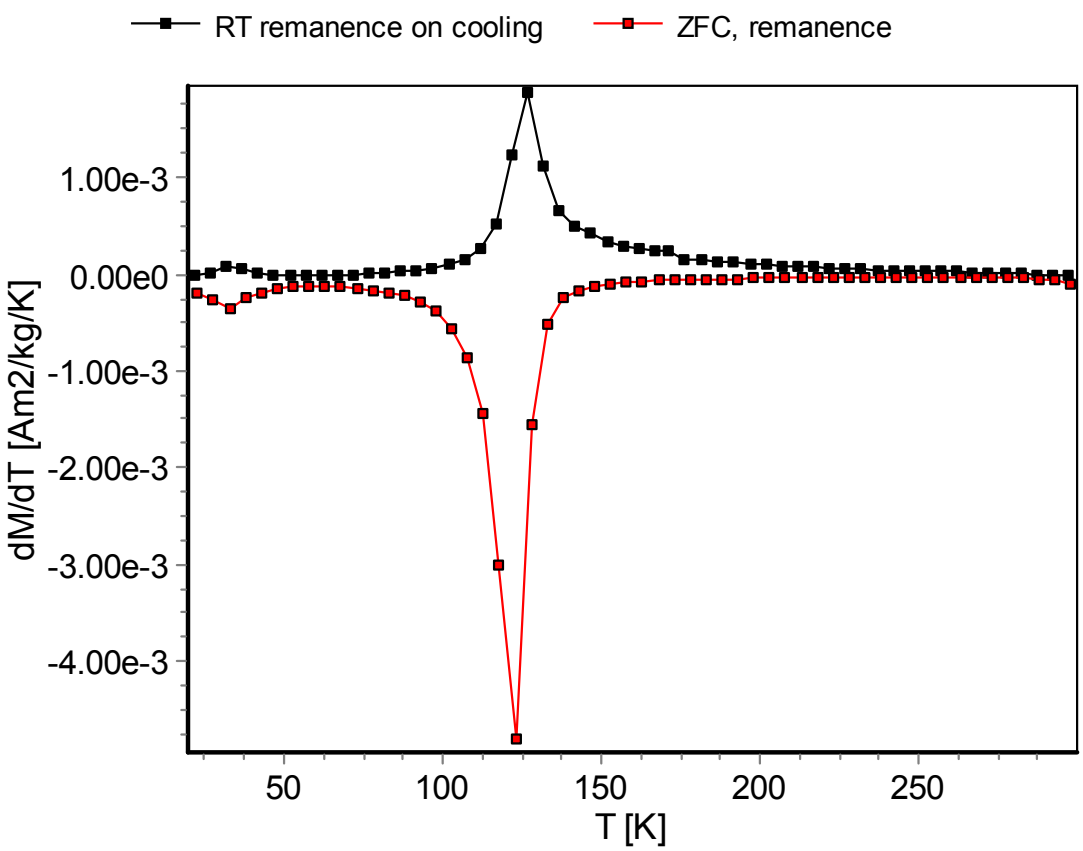

Figures 11 and 12: MPMS data from a sample in site 12. Figure B is a graph of the derivative of figure A. A dramatic loss in magnetization is visible in both the cooling and heating curves in these graphs and is centered around 120K, indicating that magnetite is present in the sample. Most of our MPMS samples showed a similar change. Another, smaller transition is visible at around 30K, which may indicate the presence of another mineral, such as pyrrhotite.

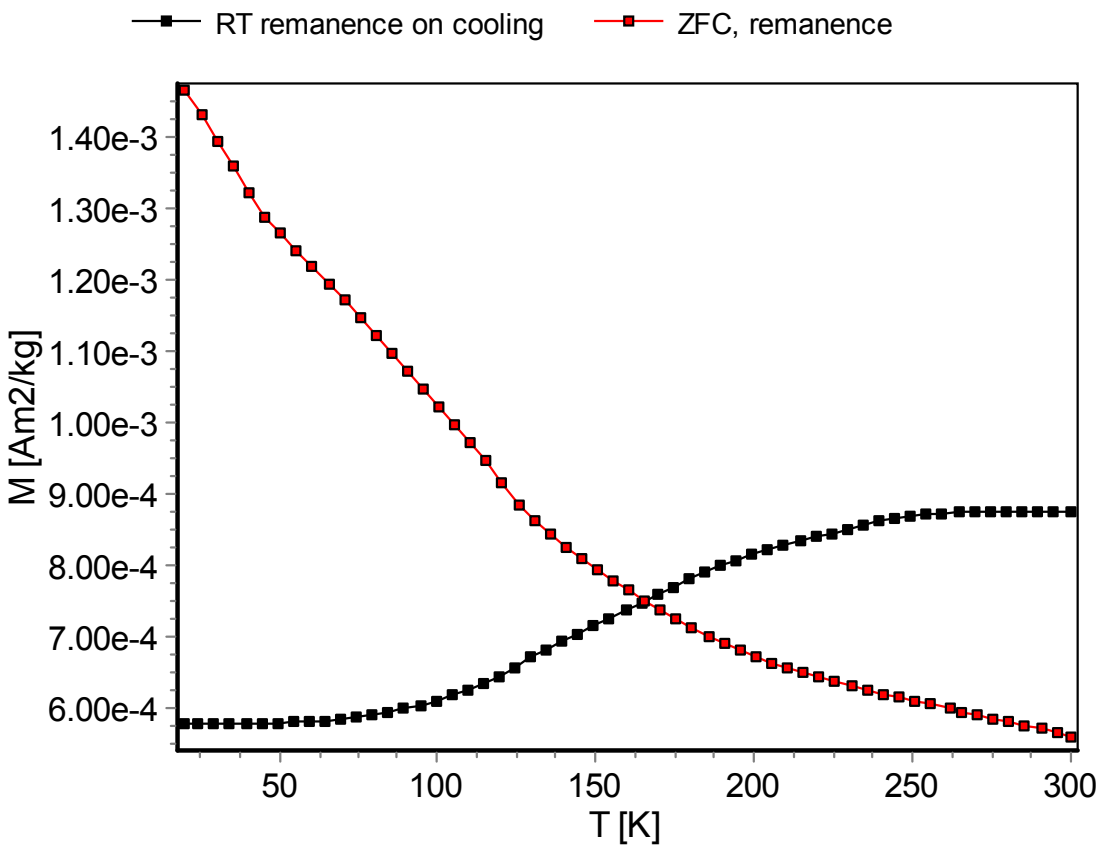

Figure 13: MPMS data from a sample in site 16. Unlike the sample from site 12, this shows a nearly negligible transition slope at 120K and may not contain a significant amount of magnetite. It is unclear whether this type of curve does indicate the presence of a particular mineral; however, there does still seem to be another very slight transition at around 30K again, possibly indicating that this sample still contains some pyrrhotite.

4.3. High-Temperature Susceptibility

Like our MPMS data, the results that we found by measuring high-temperature thermal susceptibility on our samples generally showed that a significant amount of magnetite was present. Magnetite has a Curie temperature of 580 °C, above which it cannot hold a magnetic alignment, even within a small field. Nearly all of our samples remained at a relatively consistent susceptibility for most of the experiment, but showed a sharp loss of susceptibility between 580 and 590 °C (Figure 14), again matching with what we would expect from a significant presence of magnetite (Tauxe 2014). Some samples also showed a rise and fall in

susceptibility on the heating curve, centered around 300 °C (Figure 15). Because this bump shows up in the heating curve but never the cooling curve, it may indicate the presence of another magnetic mineral that is altered upon heating, but it is unclear what mineral it likely is from the current literature.

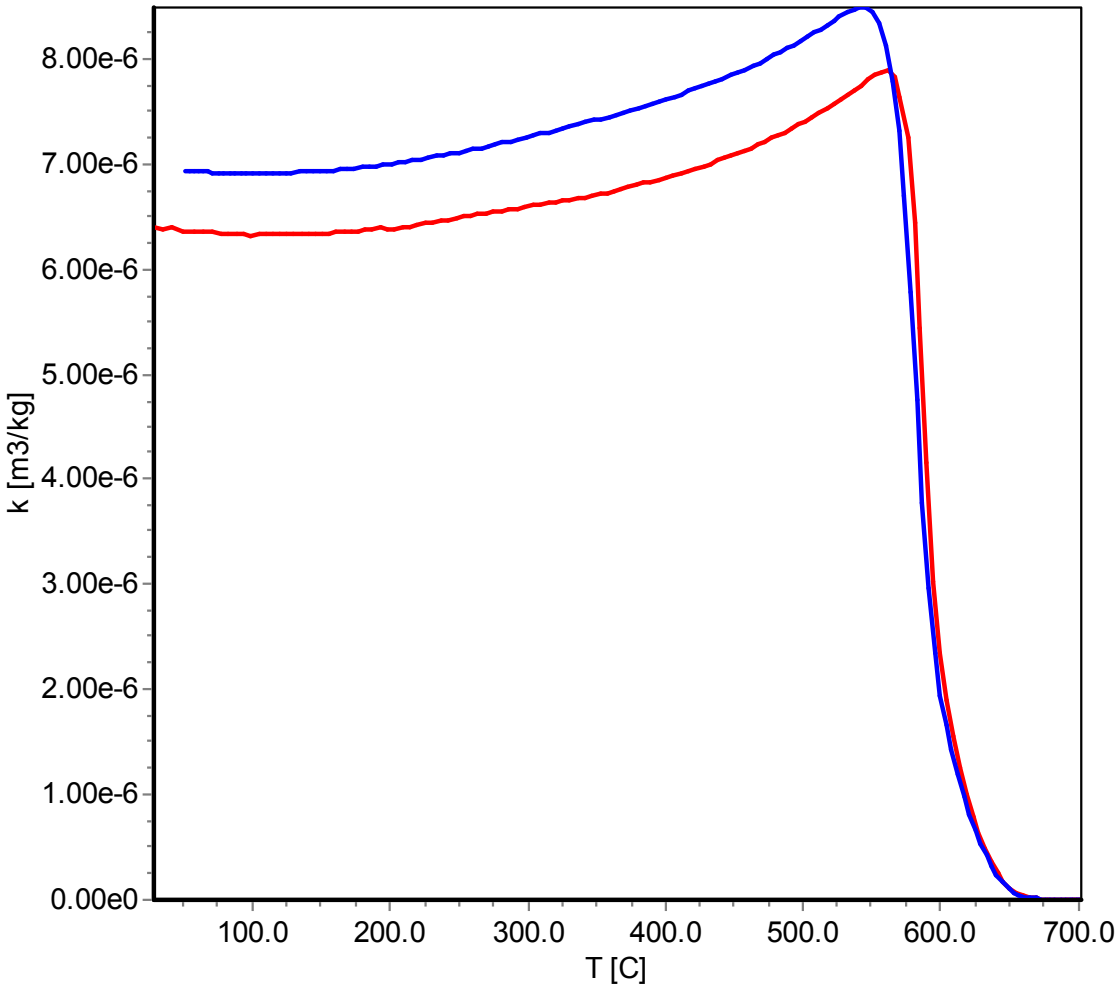

Figure 14: kT data from a sample in site 4. This graph is a very clear example of the behavior of magnetite upon heating (red curve) to the Curie temperature of about 580-590 C. Above the Curie temperature, the magnetite loses its magnetic susceptibility, then regains it upon cooling (blue curve) back below the same point.

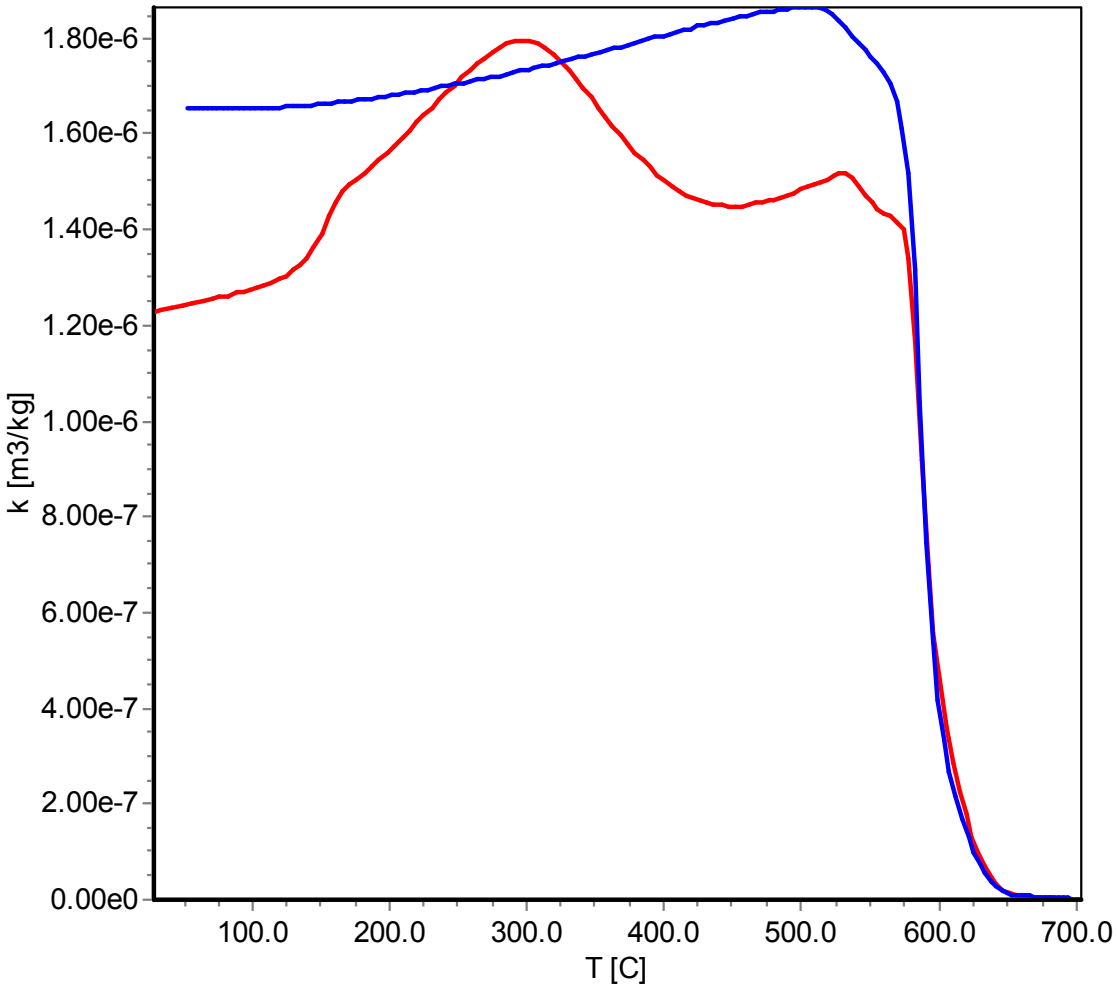

Figure 15: kT data from a sample in site 17. Like the data from site 15, this shows a dramatic loss of susceptibility above the magnetite Curie temperature, indicating the presence of magnetite in the sample. However, it also shows a bump in susceptibility in the heating curve, possibly indicating the presence of another magnetic mineral.

4.4. Hysteresis

Using the Mr/Ms and Hci/Hc values from each of our hysteresis loops, we were able to place each of our samples on a Day diagram (Day, 1977) to determine roughly whether our magnetite crystals could be classified as single-domain (SD), multi-domain (MD), or pseudo-single-domain (PSD). The size boundaries between SD, PSD, and MD crystals are not entirely consistent, but the minimum width of MD magnetite crystals is estimated to be about 10-20 μm. As is very common for

hysteresis experiments done on rock samples, the hysteresis loops of our samples showed that the magnetic grain size almost always fell in the pseudo-single-domain range (Figure 16). This result can indicate either that most of the magnetic grains really are in the pseudo-single-domain size range, or that there is a mix of single-domain and multi-domain grains present.

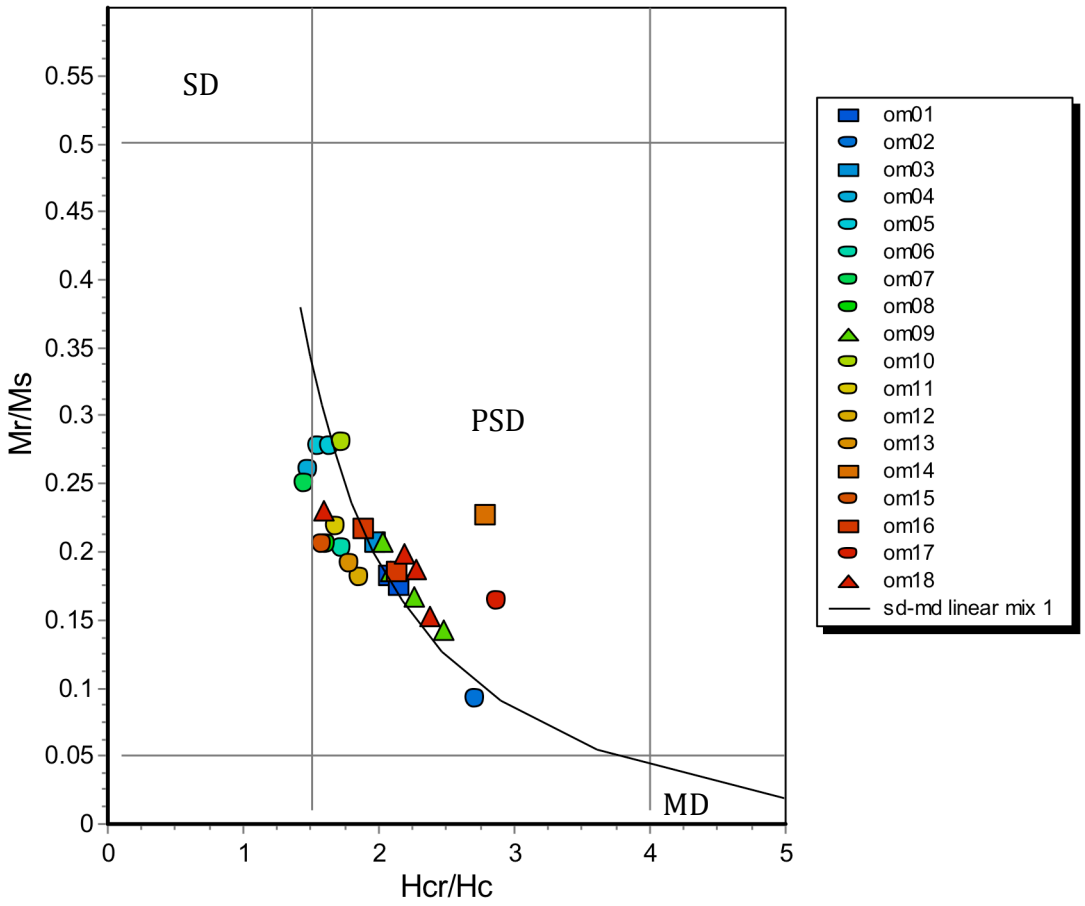

Figure 16: A Day diagram summarizing all of our hysteresis results. Samples with Mr/Ms > 0.5 and Hcr/Hc <1.5 are considered to be SD, those with 0.05 < Mr/Ms < 0.5 and 1.5 < Hcr/Hc < 4 are PSD, and those with Mr/Ms < 0.05 and Hcr/Hc > 4 are MD. Our sample points are generally shown to lie in the PSD range near an SD-MD mixing line. Sites determined to have significantly less magnetite from their low-temperature magnetization data (1, 3, 14, and 16) are marked as squares, and sites with multiple samples tested (9 and 18) are marked as triangles. The trend line is a model for linear mixes of SD and MD magnetite grains from Dunlop (2002).

4.5. Thin section analysis

Our samples contain a majority of plagioclase, with a noticeable amount (roughly 10-20% each) of clinopyroxene and olivine. There are visible preferred crystal orientations at the thin section scale, and separate layers of olivine and plagioclase are visible in both hand sample and thin section. The olivine has consistently been somewhat altered and often has serpentine rims of varying degrees. Cracks within the olivine crystals consistently contain opaque minerals (Figure 17). The clinopyroxene does not appear to have been noticeably altered and is not associated with serpentine, nor does it have any fractures containing opaques, although more heavily weathered ophiolite samples have been observed to contain altered pyroxene (Yaouancq and MacLeod, 2000).

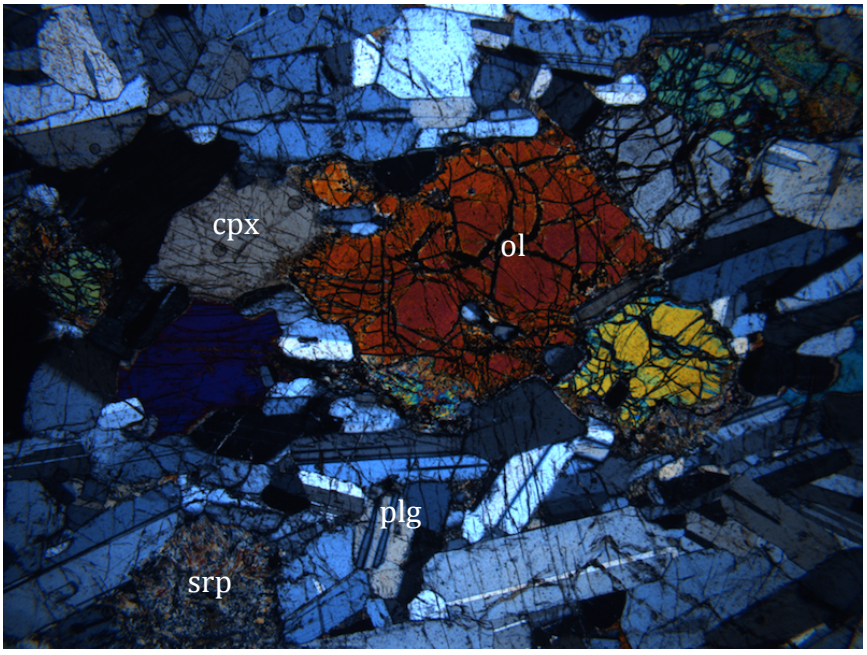

Figure 17: Image of a thin section taken from site 10. The more brightly colored, fractured crystals are olivine, with darker clinopyroxene crystals to the left and light grey, more rectangular plagioclase all around. Some serpentine alteration is visible on the bottom edges of the olivine and near the lower-left corner of the image. A rough trend in plagioclase crystal orientations is also visible from this image. Preferred crystal orientations and compositional layering between plagioclase and olivine are what generally define the visible fabric at thin-section scale. Field of view is about 5 mm across.

Examination of thin sections of our samples with reflected light microscopy shows us that much of the magnetite present in the gabbros is located within altered fractures in and rims around the olivine crystals (Figure 18). There are also less common, slightly larger blobs of magnetite around the more altered edges of the olivine grains, but these do not appear to have any particular directional preference. These results suggest that the AMS fabric directions are largely dependent on the alignment of the secondary magnetite in the altered olivine crystals.

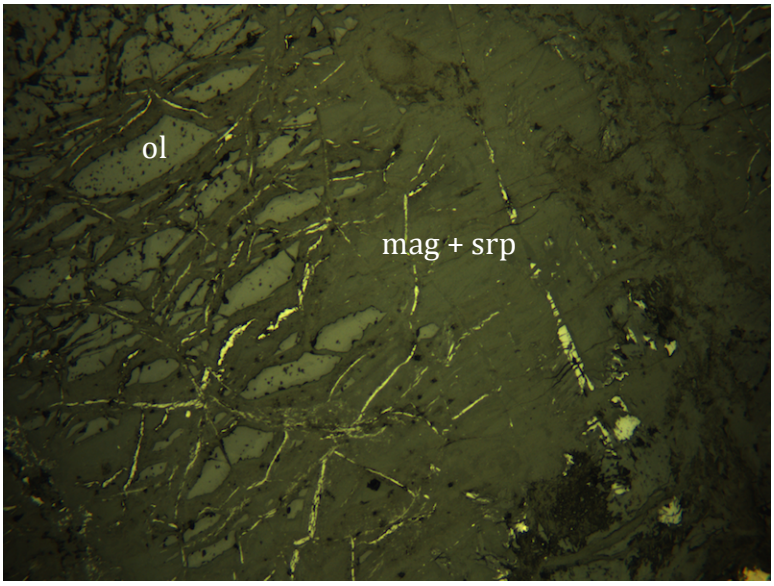

Figure 18: Reflected light image of the edge of a weathered olivine crystal. The cracks in the olivine are visible and bright magnetite veins can be seen following them and tracing out a skeleton of the olivine. Alteration like this is likely a significant control on the AMS directions in our samples. Field of view is 1 mm across.

We also observed several opaque minerals in our samples other than magnetite, which may have been the cause of some of the unexpected variation in kT and MPMS results. These minerals were often associated with each other outside of the olivine crystals, and were thus likely primary and not due to alteration of the other minerals (Figure 19). Their overall contribution to the AMS directions and other magnetic results is unclear.

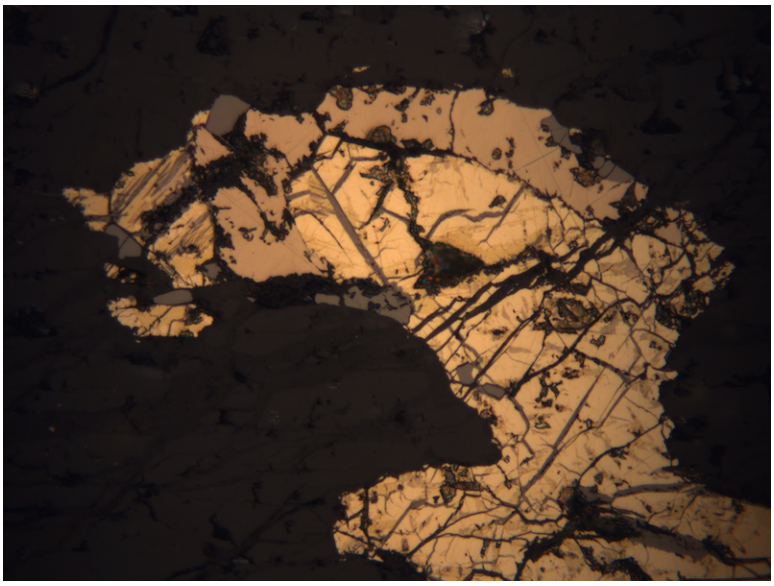

Figure 19: A reflected light image of a few associated opaque minerals from a thin section in site 5, some of which were only observed in larger blobs like this one, rather than in fractures in the olivine. Field of view is about 250 microns across.

Our SEM results confirm that the thin opaque crystals inside alteration fractures in the olivine are almost entirely magnetite, with rare sulfide crystals in the larger, more heavily altered areas. There is always serpentine present on either side of the magnetite (Figure 20). The two likely formed at the same time, since they both result from alteration of olivine and are often associated with each other in altered olivine fractures (Delvigne et. al., 1979). We also used the SEM to identify the opaque minerals that we saw in thin section, and discovered that, along with magnetite, there were Fe, Ni, and Cu sulfides present in some of our samples (Figure 21).

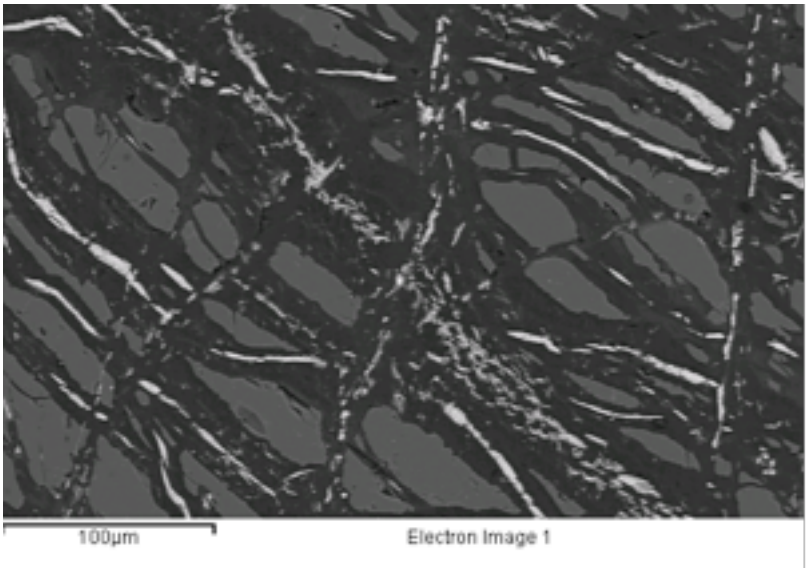

Figure 20: A BSE image of an olivine grain with (darker) serpentine and (brighter) magnetite alteration fractures. Within the olivine crystals, the magnetite is always bordered by serpentine on either side.

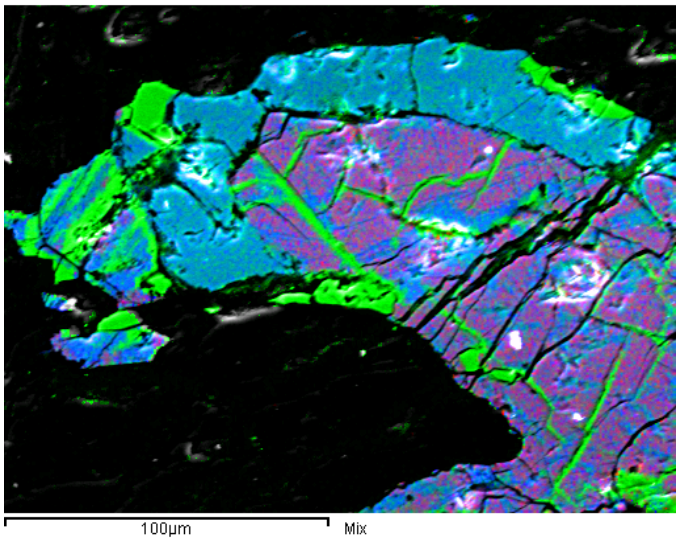

Figure 21: An element map of the group of associated opaque minerals from Figure 19. Here, iron is green, sulfur is blue, and nickel is red. The bright green veins seen here are magnetite, the blue-green mineral is pyrrhotite (an iron sulfide) and the purple is likely pentlandite (a nickel sulfide).

5. Site Results

There seemed to be a fairly consistent pattern in the results that we found in each of our sites. Overall, it seemed that sites with a significant magnetite content tended to also have more consistent AMS directions, both within and between sites.

Relative magnetite content was judged both from trends in low-T magnetization and high-T susceptibility data and by direct observation in thin section.

5.1. Site 5

The AMS data from site 5 (Figure 22a) was very consistent, both with the AMS data from most of the other sites and with its plagioclase and opaque mineral shape-preferred orientations (Figs. 22b and 22c). Both its low-temperature magnetization and high-temperature susceptibility data (Figs 22d and 22e) indicate the presence of magnetite (by the 120K Verwey transition and 580-590 °C Curie temperature, respectively), and a significant amount of altered olivine was observed in all of its thin sections, along with some accessory sulfides.

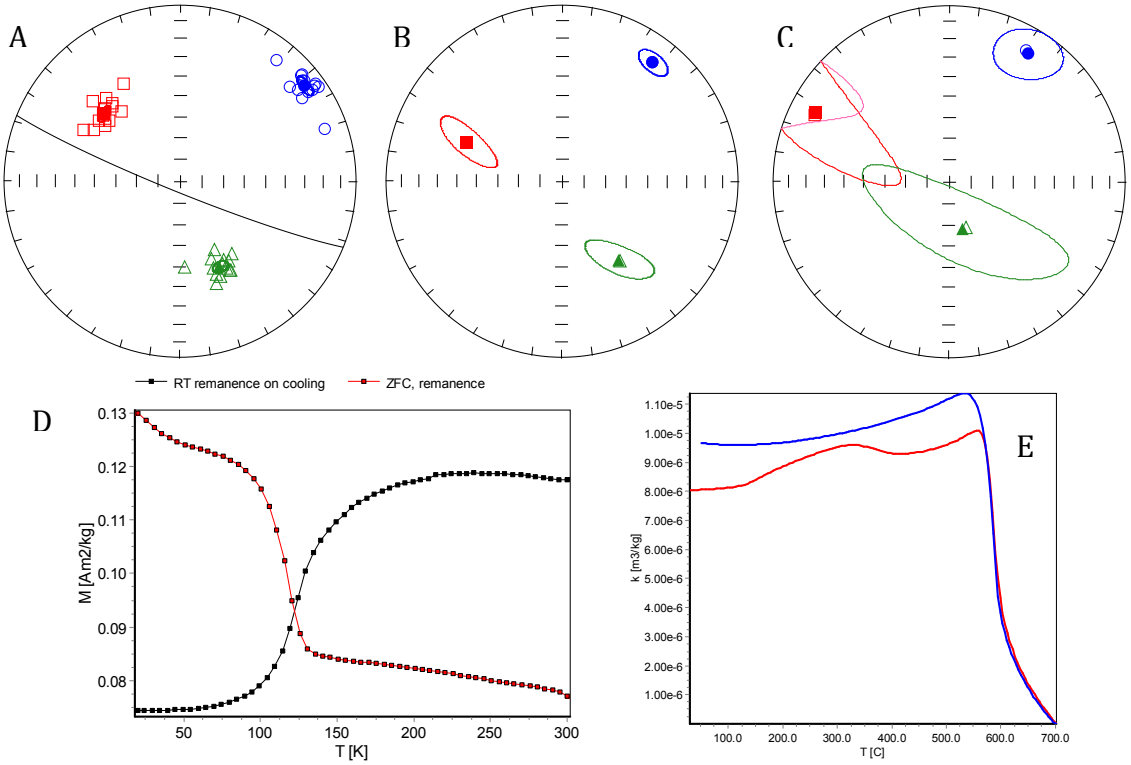

Figure 22: The AMS (A), SPO (B and C), low-T magnetization (D), and high-T susceptibility (E) data from site 5. The AMS data includes the orientation of the foliation plane observed in the field for this site.

5.2. Site 15

Much like site 5, the magnetic data for site 15 indicated a significant presence of magnetite, and its AMS data was consistent with most of the other sites. Its mineral SPO data somehow has the Kmax and Kint directions switched, and it is unclear why the two fabric measurements show a different lineation, but the foliation is still roughly the same.

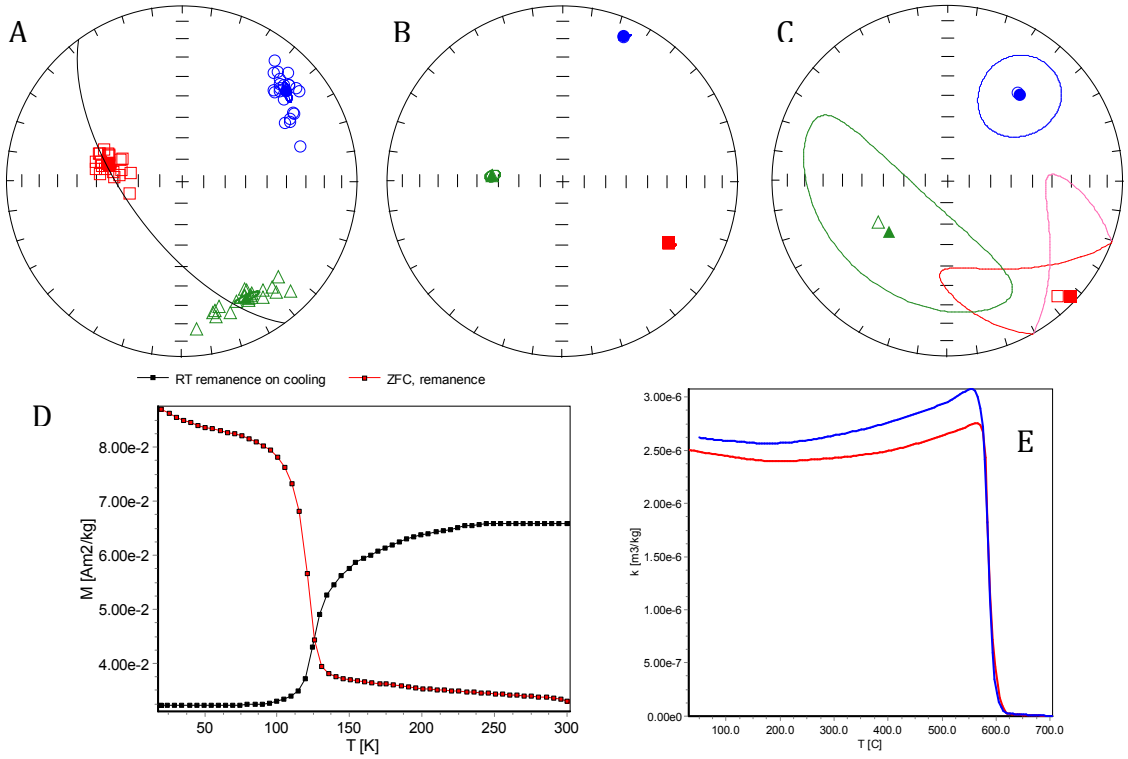

Figure 23: The AMS (A), SPO (B and C), low-T magnetization (D), and high-T susceptibility (E) data from site 15.

5.3. Site 9

Site 9 was one of two sites (along with 18) that had its AMS results roughly split in half by whether their Kmax and Kint directions would be consistent with most of the other sites (Kmax plunging to the northwest) or flipped. Its low-temperature magnetization (Figure 24b) does seem to indicate the presence of

magnetite, but the transition is less clear than in sites 5 and 15. Likewise, its high-temperature susceptibility data is odd in that it does not show a clear loss of susceptibility right at the Curie temperature; instead, the susceptibility seems to trail off. One thin section was made and observed for site 9, and the presence of olivine and magnetite was relatively small (~3% olivine by area).

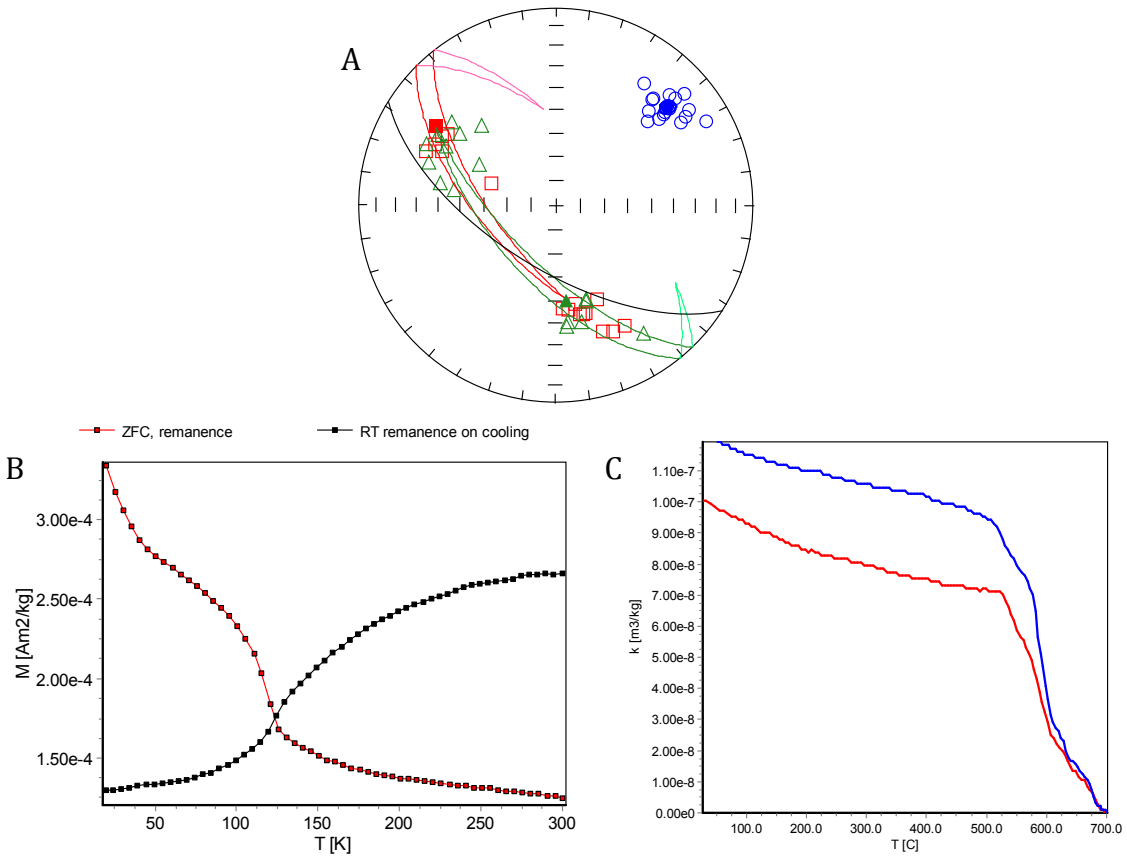

Figure 24: The AMS (A), low-T magnetization (B), and high-T susceptibility (C) data from site 9.

5.4. Site 14

Site 14 has another set of behaviors that is unusual for our data. The Kmax and Kint directions on the AMS diagram seem to be rotated from the main clusters shown in Figure 7b, although the AMS data still seem to stay close to the foliation observed in the field. The low-temperature magnetization data does not seem to show a Verwey transition at all, and the high-temperature susceptibility data seems

to have changes at a range of temperatures outside of the Curie temperature for magnetite. We were not able to determine for certain what mineral was causing the different patterns in these data, but it did not seem like the dominant magnetic phase was magnetite.

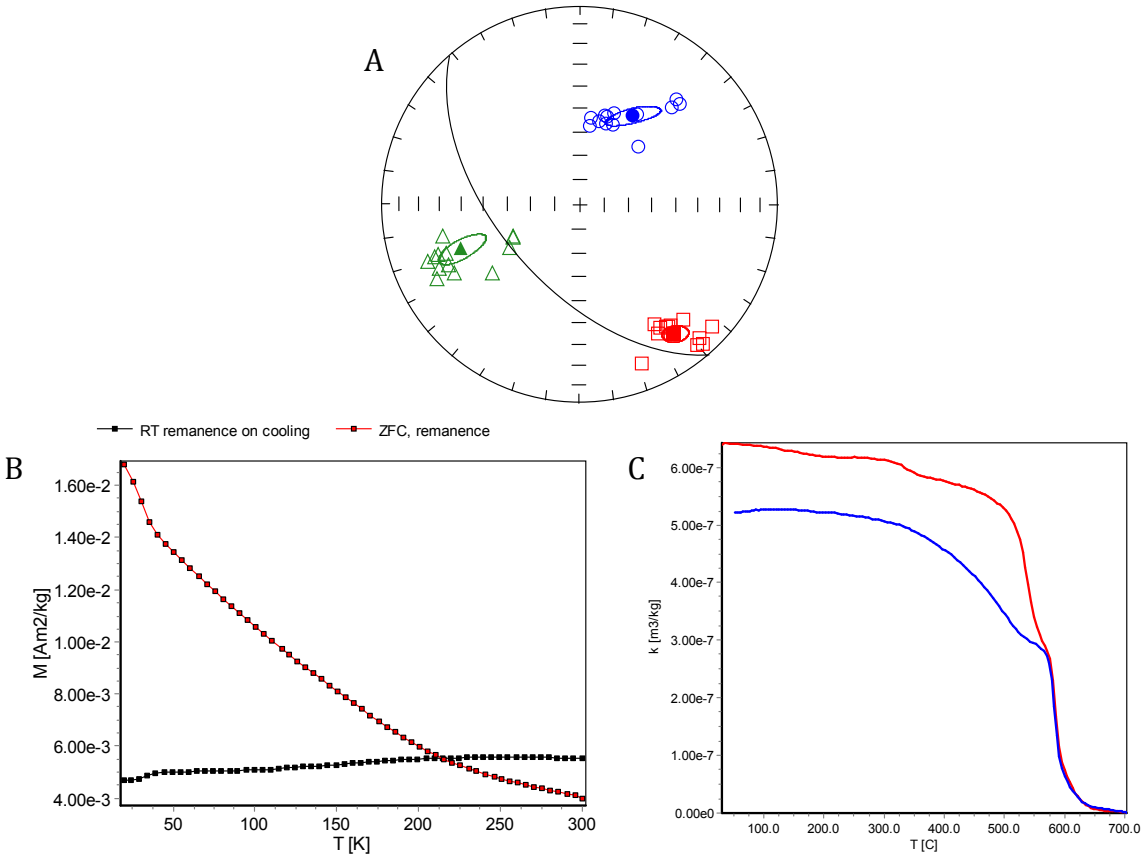

Figure 25: The AMS (A), low-T magnetization (B), and high-T susceptibility (C) data from site 14.

6. Discussion

It is useful to consider the mineral assemblage and alteration history of the Oman ophiolite when interpreting the AMS fabrics in our samples; in particular, the presence of olivine in the foliated gabbros had a significant effect on our AMS results. When olivine undergoes low-temperature (<400 C) hydrothermal alteration, it undergoes a reaction with water to form serpentine, magnetite, and hydrogen gas:

$$(Fe,Mg)_2SiO_4 + H_2O \rightarrow Mg_3Si_2O_5(OH)_4 + Fe_3O_4 + H_2$$

(Delvigne et. al., 1979; Yaouancq and MacLeod, 2000). This reaction most likely occurred with seawater while the ophiolite was still located on the seafloor, but its exact timing is unclear. As we observed in our thin sections, this reaction tends to leave thin veins of magnetite with serpentine on either side; the alteration pattern follows existing fractures in the olivine. If these fractures are random, then the resulting serpentine-magnetite skeleton will likely trace out the overall shape of the olivine crystal. Olivine can also be associated with primary magnetite in igneous rocks, as well as other ores such as titanomagnetite, ilmenite, and Fe-Ni-Cu sulphides (Delvigne et. al., 1979).

Considering that the magnetite in our samples appears to be largely due to alteration of olivine and did not crystallize from the original magma, it is interesting that our AMS results show any consistent directions at all, let alone ellipsoid axes that are so consistent and match so closely with our rock fabric orientations. However, given that the directions within each site are so consistent throughout nearly all of our data, it would make sense for there to be some kind of pattern for the magnetic minerals to follow, because the results are very clearly not random. One possibility is that the alteration fractures in the olivine are randomly oriented overall, which could mean that the alignment of the secondary magnetite depends on either the shape-preferred orientation of the olivine crystals or their compositional layering within the gabbros. Another possibility pointed out by Yaouancq and MacLeod (2000) is that the fractures in the olivine are not random, but instead follow the overall rock fabric, since foliation planes in the gabbros could

have provided planes of relative weakness along which water could flow during the serpentinization process. This scenario would mean that the AMS fabric would be dependent on the overall foliation orientations in the rock rather than the alignment of only the olivine crystals. Unfortunately, the difference between these two scenarios is subtle in terms of results and the data from this project does not seem to be enough to distinguish between them, so whether Yaouancq and MacLeod were right is difficult to say. However, they and others (Luyendyk and Day, 1982; Kawamura et. al., 2005) do agree with our conclusion that the magnetic fabric of the foliated gabbros is largely due to the presence of secondary magnetite.

7. Conclusion

Upon measuring both the AMS and visual fabrics in our samples, we found that the two did coincide and that AMS is a useful method for studying magma flow directions in these rocks. Data taken at the Institute for Rock Magnetism show that the AMS signal is largely due to magnetite, with a possible minor presence of other magnetic minerals. Thin sections taken from our samples show us that much of the magnetite present is likely due to serpentinization and secondary mineralization from the olivine in the gabbros, suggesting that the presence of olivine is necessary for the magnetic fabric to be clear and consistent. Our AMS directions are likely due to the fact that the magnetite roughly imitates either the shape of the olivine crystals or the foliation planes in the rock. Either way, the overall alignment of the magnetite matches the directions of the primary rock fabric.

Our AMS fabric directions are remarkably consistent and show a foliation (Kmax-Kint plane) direction that largely matches both the mesoscopic foliations

measured in the field and the trend of the nearby inferred ridge axis, with a magnetic lineation (Kmax direction) that moderately plunges toward the Maqsad diapir to the northwest. The foliation is dipping steeply to the southwest, away from the inferred ridge, since the study site is just to the south of it. The fabric directions from this site suggest that magma was being pushed up and out from the diapir along the ridge axis.

8. Acknowledgements

Many thanks to my research advisor, Andrew Horst, for letting me join this project and for his encouragement, insight, and unending patience. A huge thank you to Yumi Ijiri, Zeb Page, and Steve Wojtal for their comments and advice, and for teaching me so much over the last few years. I want to give special thanks to my family for their love and support, and to the Oberlin Geology department for an amazing education with fun, fantastic people. I also thank Jeff Gee at Scripps Institute of Oceanography and Mike Jackson, Dario Bilardello, and Joshua Feinberg at the Institute for Rock Magnetism for their help gathering and understanding our magnetic data. Also thanks to Dr. Mohammad Al Battashi at the Sultanate of Oman Ministry of Commerce and Industry for assistance with permission to collect samples and Dr. Sobhi Nassir at the Sultan Qaboos University for additional field logistical support. The fieldwork and other travel costs for this project were supported by Oberlin College Grant-In-Aid, and Powers Travel Grant.

9. References

Abelson, M., Baer, G., and Agnon, a, 2001, Evidence from gabbro of the Troodos ophiolite for lateral magma transport along a slow-spreading mid-ocean ridge.: Nature, v. 409, p. 72–75, doi: 10.1038/35051058.

Archanjo, C.J., Campanha, G. a C., Salazar, C. a., and Launeau, P., 2012, Using AMS combined with mineral shape preferred orientation analysis to understand the emplacement fabrics of the Apiai gabbro-norite (Ribeira Belt, SE Brazil): International Journal of Earth Sciences, v. 101, p. 731–745, doi: 10.1007/s00531-011-0659-x.

Bilardello, D., and Jackson, M., 2013, What do the Mumpsies do?: The IRM Quarterly, v. 23, p. 1, 11-15

Boudier, F., Nicolas, A., and Ildefonse, B., 1996, Magma chambers in the Oman ophiolite: fed from the top and the bottom: Earth and Planetary Science Letters, v. 144, p. 239–250.

Christensen, N.I., and Smewing, J.D., 1981, Geology and seismic structure of the northern section of the Oman ophiolite: Journal of Geophysical Research: Solid Earth, v. 86, p. 2545–2555, doi: 10.1029/JB086i

Collier, J.S., and Singh, S.C., 1997, Detailed structure of the top of the melt body beneath the East Pacific Rise at 9 40'N from waveform inversion of seismic reflection data: Journal of Geophysical Research, v. 102, p. 287–304.

Day, R., Fuller, M., and Schmidt, V.A., 1977, Hysteresis properties of titanomagnetites: grain-size and compositional dependence: Phys. Earth\rPlanet. Inter., v. 13, p. 260–267.

Delvigne, J., Bisdom, E.B.A., Sleeman, J., and Stoops, G., 1979, Olivines, their Pseudomorphs and Secondary Products: Pedologie, v. 29, p. 247–309.

Granot, R., Abelson, M., Ron, H., Lusk, M.W., and Agnon, A., 2011, Direct evidence for dynamic magma supply fossilized in the lower oceanic crust of the Troodos ophiolite: Geophysical Research Letters, v. 38, p. 2–7, doi: 10.1029/2011GL048220.

Hrouda, F., 1982, Magnetic anisotropy of rocks and its application in geology and geophysics: Geophysical Surveys, v. 5, p. 37–82, doi: 10.1007/BF01450244.

Kawamura, K., Hosono, T., Allawati, H.M., Ogawa, Y., and Taniguchi, H., 2005, Origin of layering in cumulate gabbros in the Oman ophiolite: Insights from magnetic susceptibility measurements in the Wadi Sadm area: Island Arc, v. 14, p. 564–570, doi: 10.1111/j.1440-1738.2005.00484.x.

Kelemen, P.B., Koga, K., and Shimizu, N., 1997, Geochemistry of gabbro sills in the crust-mantle transition zone of the Oman ophiolite: implications for the origin of the oceanic lower crust: Earth and Planetary Science Letters, v. 146, p. 475–488, doi: 10.1029/97JB02604.

Luyendyk, B.P., and Day, R., 1982, Paleomagnetism of the Samail Ophiolite, Oman: 2. The Wadi Kadir Gabbro Section: Journal of Geophysical Research, v. 87, p. 10,903–10,917.

MacLeod, C.J., Johan Lissenberg, C., and Bibby, L.E., 2013, "Moist MORB" axial magmatism in the Oman ophiolite: The evidence against a mid-ocean ridge origin: Geology, v. 41, p. 459–462, doi: 10.1130/G33904.1.

Nicolas, A., Boudier, F., and France, L., 2009, Subsidence in magma chamber and the development of magmatic foliation in Oman ophiolite gabbros: Earth and Planetary Science Letters, v. 284, p. 76–87, doi: 10.1016/j.epsl.2009.04.012.

Searle, M., and Cox, J., 1999, Tectonic setting, origin, and obduction of the Oman ophiolite: Bulletin of the Geological Society of America, v. 111, p. 104–122, doi: 10.1130/0016-7606(1999)111<0104:TSOAOO>2.3.CO;2.

Sinton, J.M., and Detrick, R.S., 1992, Mid-ocean ridge magma chambers: Journal of Geophysical Research, v. 97, p. 197, doi: 10.1029/91JB02508.

Tarling, D.H., and Hrouda, F., 1993, The magnetic anisotropy of rocks: London, Chapman & Hall.

Tauxe, L, Banerjee, S.K., Butler, R.F. and van der Voo R, Essentials of Paleomagnetism, 3rd Web Edition, 2014.

VanTongeren, J. a., Hirth, G., and Kelemen, P.B., 2015, Constraints on the accretion of the gabbroic lower oceanic crust from plagioclase lattice preferred orientation in the Samail ophiolite: Earth and Planetary Science Letters, v. 427, p. 249–261, doi: 10.1016/j.epsl.2015.07.001.

Yaouancq, G., and MacLeod, C.J., 2000, Petrofabric investigation of gabbros from the Oman ophiolite: Comparison between AMS and Rock Fabric: Marine Geophysical Researches, v. 21, p. 289–305, doi: 10.1023/A:1026774111021.